Implementation Options of Control Systems for a Cantilever Calibration Device

Valeriya A. Cherkasova
Institute of Process Measurement and Sensor Technology
Technische Universität Ilmenau
Ilmenau, Germany
valeriya.cherkasova@tu-ilmenau.de

Thomas Froehlich
Institute of Process Measurement and Sensor Technology
Technische Universität Ilmenau
Ilmenau, Germany
thomas.froehlich@tu-ilmenau.de

***Аннотация*. В статье описаны глобальные подходы к управлению устройством калибровки кантилевера. Идея устройства заключается в электромагнитной компенсации влияния консольных сил. Разработка регуляторов основана на моделировании механических процессов при воздействии кантилевера на ячейку нагрузки с принципом электромагнитной компенсации, выполнена идентификация процессов. Также в ходе исследования проводилось сравнение ПИД-регуляторов, реализованных на различных системах воздействия: аналоговой схеме, источнике тока, системе реального времени dSPACE, микроконтроллере. Целью разработки и сравнения регуляторов было улучшение показателей качества управления: времени регулирования, перерегулирования, амплитуды шума.**

Ключевые слова: система управления, ПИД-регулятор, микроконтроллер, система реального времени, калибровка, кантилевер, компенсация электромагнитных сил

I. Introduction

Since 1986, when the first experimental implementation of an atomic force microscope was made, the measurement resolution has significantly decreased from nanometers to picometers. Achievement of such a resolution became possible due to the precision calibration of the cantilever. It is essential for accurate AFM measurements and quantitative analysis. In addition, calibration should not degrade the tip.

There are various groups of cantilever calibration methods: dimensional, internal, dynamic, static. The smallest measurement uncertainty was achieved using the static method. Based on this method, a displacement force measuring device for determining the spring stiffness was developed at the Technical University of Ilmenau [1]. The study was continued and a test bench was developed for traceable calibration of cantilevers [2], the result of the study was the relative measurement uncertainty of the soft cantilever calibration of 1.5 % (k = 2) with a calibration force <100 nN.

Improvement of the presented results can be achieved by changing the executive servo-control mechanisms depending on the input signals for the control device and the capabilities of analog and digital control.

The authors gratefully acknowledge the support by the Deutsche Forschungsgemeinschaft (DFG) in the scope of the Research Training Group "Tip- and Laserbased 3D-Nanofabrication in extended macroscopic working areas" (GRK 2182) at Technische Universität Ilmenau, Germany.

II. The Controlled Test Stand for Calibrating Cantilevers and Principle of Operation

The functional principle of the device is based on electromagnetic force compensation (EMFC). The main advantage of EMFC is linearity. This principle is widely used in the field of precision weighing [3]–[5]. Controlled test stand for calibrating cantilevers is shown in Fig. 1 [2].

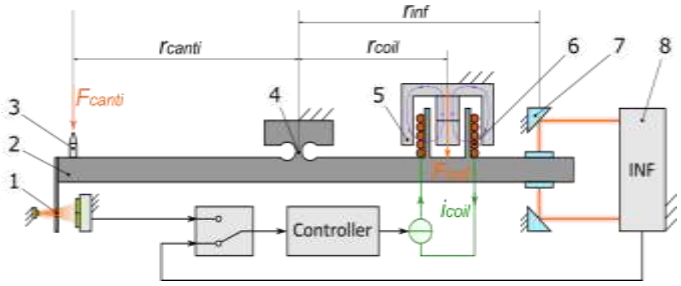

Fig. 1. Controlled test stand for calibrating cantilevers with: (1) slit aperture; (2) beam balance; (3) push button; (4) joint; (5) permanent magnet; (6) coil; (7) deflection mirror; (8) interferometer

The impact of the cantilever on diamond push button creates a deflection of the balance beam, the deflection is recorded by two different position sensors: a slit aperture with differential photodiodes and an interferometer. The use of to position sensors is due to the absence of absolute zero when using an interferometer. Deflection of the balance can be interpreted via voltage or digital incremental quadrature signal. A coil is attached to the balance in a constant magnetic field. By regulation the coil current, the balance returns to the zero position and the force of the cantilever can be calculated through a linear relationship:

$$F_{canti} = \frac{B \cdot l \cdot r_{coil}}{r_{canti}} \cdot i_{coil} \qquad (1)$$

where B – magnetic-flux density, l – the length of the coil.

In accordance with the schematic diagram of the experimental setup, global types of control are subdivided into three:

1) input signal from slit aperture;
2) input signal from interferometer;
3) both input signals.

The possibilities of using the various position sensors provided in the installation allow testing the capabilities of analog and digital control. The PID algorithm was chosen to implement servo control as the most simplified comparison method.

III. Development of the Mathematical and Computer Models of Mechanical Processes in the Single Joint Load Cell

A simplified representation of the test stand is shown in Fig. 2 [6].

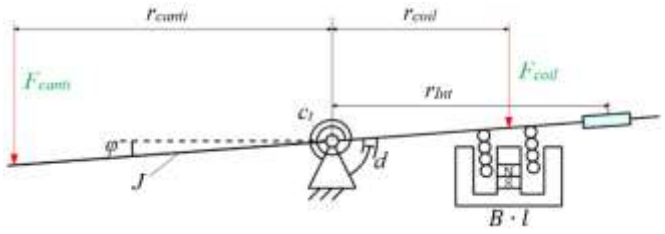

Fig. 2. Simplifed mechanical representation of the single joint load cell

In this sceme: J – moment of inertia of the beam; d – the damping coefficient of the dampfer between flexure hinge and beam; φ – the beam angular displacement; r_{Int} – the distance between mirrow of the interferometer and joint.

Based on the balance moments of forces (2) and minimum coordinates for small displacements $x = r_{Int} \cdot \varphi$, a system of differential equations is derived (3). Under the influence of the cantilever force, the cantilever stiffness coefficient is taken into account, as with the parallel connection of the springs.

$$M_J = J\frac{d^2\varphi}{dt^2}$$

$$M_d = d\frac{d\varphi}{dt}$$

$$M_c = (c_t + c_{canti}{r_{canti}}^2)\varphi \qquad (2)$$

$$M_{canti} = F_{canti}r_{canti}$$

$$M_{coil} = F_{coil}r_{coil}$$

$$M_{canti} = M_J + M_d + M_c + M_{coil}.$$

The system of equations in the canonical form of Cauchy is presented:

$$\dot{x}_1 = x_2$$

$$\dot{x}_2 = -\frac{c_t + c_{canti}{r_{canti}}^2}{J}x_1 - \frac{d}{J}x_2 + \frac{M_{canti}}{J} - \frac{M_{coil}}{J} \qquad (3)$$

Computer model is performed in the Matlab / Simulink software.

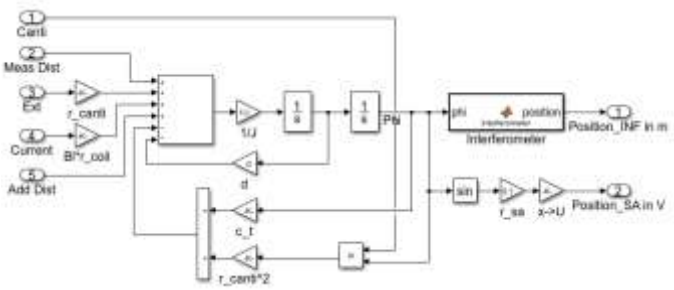

Fig. 3. Computer model of the beam balance

The model takes into account the real mechanical disturbances of the object (Fig. 4). The spectral power of real noise and simulated noise is shown in Fig. 5.

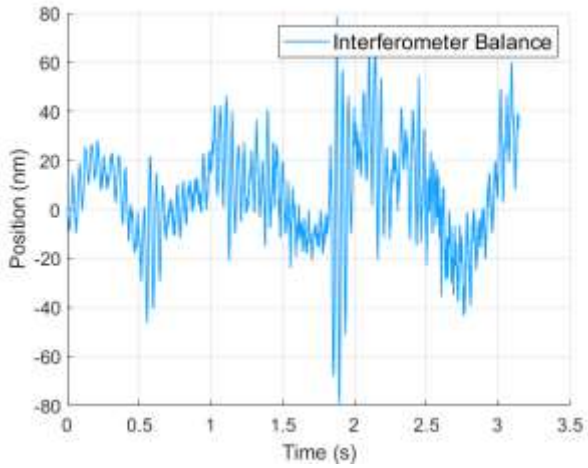

Fig. 4. Displacement of the beam with influence of the real noise

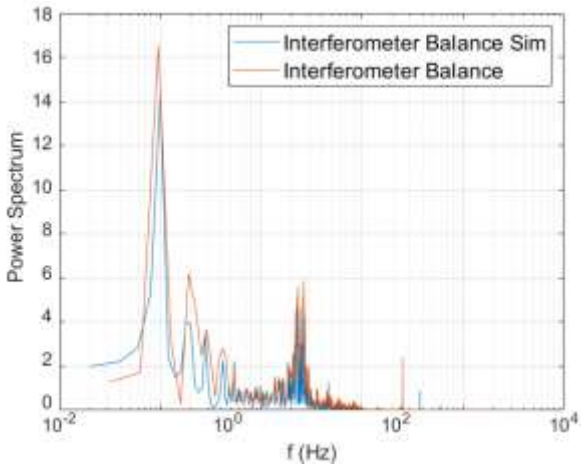

Fig. 5. Compare spectrum power of the real mechanical disturbances with simulated

Touching the cantilever beam is simulated through the step block. External exposure is represented by a pulse generator. The natural frequency of the balance is 0.934 hertz. Results of simulation without control are presented in Fig. 6.

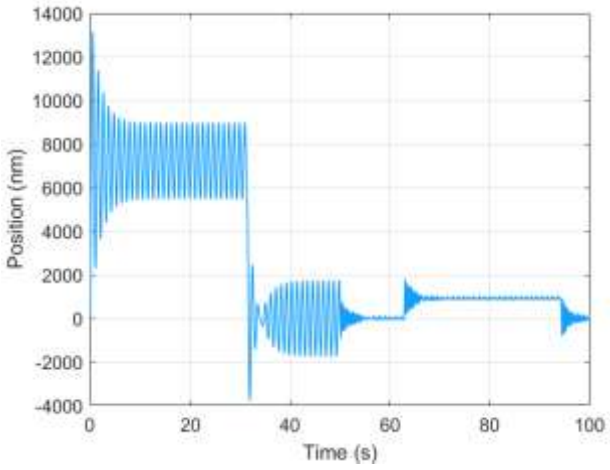

Fig. 6. Simulated displacement of the beam balance without control

IV. Comparison of PID Controllers Implemented on Various Actuator Systems

Before testing various control concepts, various actuators for a simple PID controller were tested to determine which controller is more appropriate for the future. For all actuators, the output DC current is limited to ±10 milliamperes.

A. *Current Source HP3245A*

The convenience of using a precision current source lies in the ability to program the source through the GPIB interface directly from the Matlab GUI. Fig. 7 shows a control loop using a current source and an input signal from the interferometer.

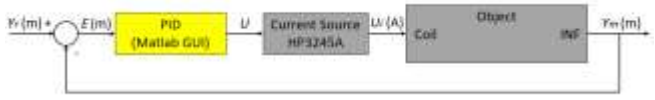

Fig. 7. Current source control loop: Y_r – reference position in meters, Y_m – measured position in meters, E – position error in meters, U – control signal (GPIB), U_i – current control signal in ampers

The sampling frequency set in the GUI is 50 hertz.

B. *Analog Circuit*

Fig. 8 shows a control loop with the implementation of the PID algorithm using operational amplifiers and an input signal from the slit aperture.

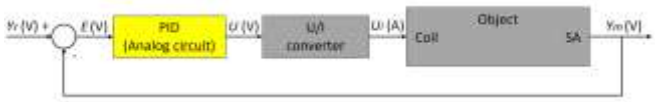

Fig. 8. Analog circuit control loop: Y_r – reference position in volts, Y_m – measured position in volts, E – position error in volts, U – voltage control signal in volts, U_i – current control signal in ampers

An analog circuit stands out for its reliability, robustness and transient process when configured well. For this, an additional analysis was carried out in the LTSpice:

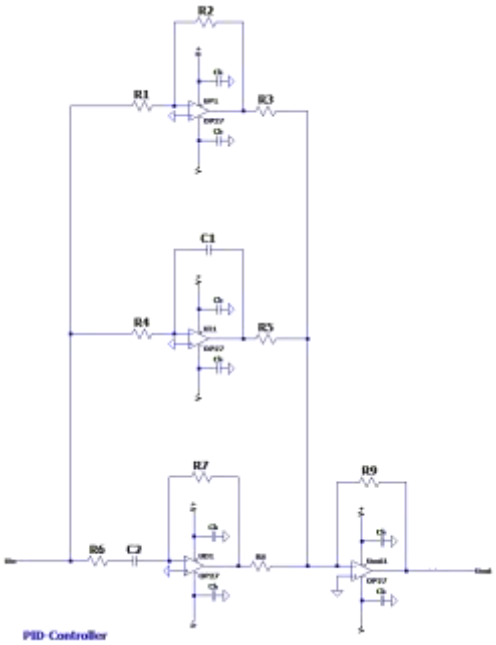

Fig. 9. PID analog circuit schematic

Accordingly, the transfer function for the analog circuit and the coefficients are expressed as follows:

$$H = P + \frac{I}{s} + \frac{DNs}{s+N} = \frac{(P+DN)s^2 + (PN+I)s + IN}{s^2 + Ns} = \frac{\left(\frac{R_2R_9}{R_1R_3} + \frac{R_7R_9}{R_6R_8}\right)s^2 + \left(\frac{R_2R_8R_9}{C_2R_1R_3} + \frac{R_9}{C_1R_4R_5}\right)s + \frac{R_9}{C_2C_1R_4R_5R_6}}{s^2 + \frac{1}{C_2R_6}s}; \quad (4)$$

$$=> N = \frac{1}{C_2R_6},$$

$$I = \frac{R_9}{C_1R_4R_5},$$

$$P = \frac{R_2R_9}{R_1R_3}, \ (R_6 = R_8) \quad (5)$$

$$D = \frac{C_2R_7R_9}{R_8}.$$

C. *DS1104 R&D Controller Board*

The advantages of using the DS1104 controller board are the convenience of embedding into a PC, which allows you to quickly create a prototype of a control system. The real-time interface provides the implementation of the Simulink model on equipment by expanding the capabilities of the C code generator. Fig. 10 describes a control loop using a controller board and an input signal from the slit aperture.

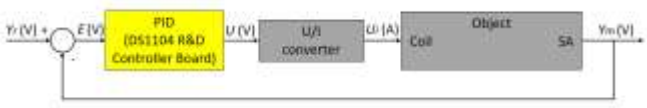

Fig. 10. DS1104 R&D controller board control loop: Y_r – reference position in volts, Y_m – measured position in volts, E – position error in volts, U – voltage control signal in volts, U_i – current control signal in ampers

D. *Microcontroller STM32F767ZI*

The advantages of the microcontroller STM32F767ZI as an actuator are the convenience of the built-in debugger/programmer, the wide range of IDE and the low cost of the board. Fig. 11 shows a control loop with a microcontroller and an input signal from the interferometer.

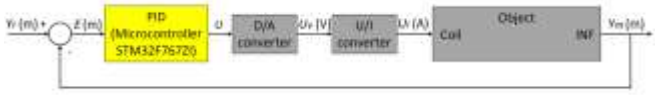

Fig. 11. Microcontroller control loop: Y_r – reference position in meters, Y_m – measured position in meters, E – position error in meters, U – control signal (SPI), U_i – voltage control signal in volts, U_i – current control signal in ampers

E. *Comparison*

Table I shows indicators for assessing the quality of the transition process. The noise indicator refers to the signal measured by the interferometer, offset is the difference in zero level of the balance when loaded and unloaded by the cantilever. Fig. 12 shows the balance deflection under the action of the cantilever for two actuators: a current source and a microcontroller.

TABLE I. COMPARISON OF THE DIFFERENT ACTUATORS

	Noise (nm)	***Overshoot (μm)***	***Regulation time (s)***	***Offset (nm)***
[1]Source	8	0.6	5	1
[2]DS1104	250	5	4.4	10
[2]Analog circuit	2.5	1.15	0.72	<1
[1]Micro-controller	0.3	0.042	0.5	-

[1]Input signal from the interferometer;
[2]Input signal from the slit aperture.

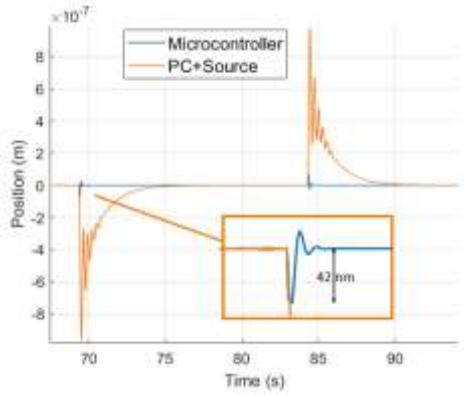

Fig. 12. Balance deflection

Based on the presented results, the best characteristics were achieved using a microcontroller and an input signal from the interferometer. There is no difference in the zero level for loading and unloading the balance by the cantilever. The noise of the measured signal is 0.3 nanometers, which is 26.7 times less than the noise when using the current source and the input signal from the interferometer, the regulation time is 10 times less and the overshoot is 14.3 times less.

V. CONCLUSION

In the course of the research, mathematical and computer models of mechanical processes in a single joint load cell were built, real mechanical disturbances were taken into account. Various actuators with a measured input signal from an interferometer or a slit aperture have been tested.

For further developments, it was decided to use the microcontroller, since the presented control characteristics can significantly improve metrological traceability. The regulation time of 0.5 second allows to reduce the time spent on the calibration of the cantilever. In addition, using a microcontroller, you can combine control for each of the input signals.

ACKNOWLEDGMENT

We thank Dr.-Ing. A. Barth, Dr.-Ing. O. Dannberg and Dipl.-Ing. G. Krapf at TU Ilmenau for their support and technical assistance.

REFERENCES

[1] Diethold C., Kühnel M., Froehlich T. "Development of a Force Displacement Measurement Device for the Determination of Spring Constants". Universitätsbibliothek Ilmenau, 2014, pp. p-10.

[2] Dannberg O., Kühnel M., Froehlich T. "Entwicklung einer Cantileverkalibriereinrichtung", tm-Technisches Messen, 87(10), pp. 622-629, https://doi.org/10.1515/teme-2020-0064, 2020.

[3] Marangoni R.R., Rahneberg I., Hilbrunner F., Theska R. and Froehlich T. "Analysis of weighing cells based on the principle of electromagnetic force compensation" Meas. Sci. Technol., 28, 75101, https://doi.org/10.1088/1361-6501/aa6bcd, 2017.

[4] Froehlich T., Rogge N., Vasilyan S., Rothleitner C., Günther L., Lin S., Hilbrunner F., Knopf D., Härtig F., and Marangoni R. "Neue Wege zur Kalibrierung von E2-Massenormalen und Darstellung von Kräften bis 10 N," tm – Technisches Messen, 87(4), pp. 280-293, https://doi.org/10.1515/teme-2019-0143, 2020.

[5] Hilbrunner F., Rahneberg I. and Froehlich T."Wattwaage mit Hebelübersetzung auf Basis eines kommerziellen EMK-Wagesystems," tm-Technisches Messen, 85(11), pp. 658-679, https://doi.org/10.1515/teme-2017-0065, 2017.

[6] Cherkasova V., Dannberg O., Froehlich T. "A Control Concept of a Compensation Load Cell in Terms of Calibration a Cantilever," in Proc. of the SMSI 2021 Conference, May 2021, digital, pp. 59-60. Available: AMA, https://www.ama-science.org [Accessed: 30 June. 2021].

[7] Shaw G.A. "Current state of the art in small mass and force metrology within the International System of Units." Measurement Science and Technology 29.7 (2018): 072001.